

Influence of the Chain Length on the Thermal Behavior of Lanthanide(III) 4-Alkoxybenzoates

Liesbet Jongen,[†] Bart Goderis,[†] Igor Dolbnya,[‡] and Koen Binnemans^{*,†}

Department of Chemistry, Katholieke Universiteit Leuven, Celestijnenlaan 200F, B-3001 Leuven, Belgium, and DUBBLE-CRG/ESRF, Rue des Martyrs 156, B. P. 220, F-38043 Grenoble Cedex, France

Received June 27, 2002. Revised Manuscript Received August 26, 2002

4-Alkoxybenzoic acids are well-known liquid crystals. The rigid core of the mesogen is formed by intermolecular hydrogen bonds. Layered structures with characteristics that depend on the lanthanide ion are formed when a trivalent lanthanide ion is introduced. Also, the chain length influences the structure and hence the thermal behavior of these complexes. Lanthanide complexes of 4-butyloxybenzoic acid have a low crystallinity, whereas metal complexes with longer chain lengths display several types of layered structures. The thermal behavior of lanthanum(III) and holmium(III) 4-butyloxybenzoate, 4-hexyloxybenzoate, 4-octyloxybenzoate, 4-nonyloxybenzoate, and 4-decyloxybenzoate is discussed, relying on differential scanning calorimetry (DSC), thermooptical microscopy, and synchrotron X-ray diffraction data. A smectic A mesophase was observed for lanthanum(III) 4-hexyloxybenzoate, lanthanum(III) 4-octyloxybenzoate, and lanthanum(III) 4-nonyloxybenzoate. The corresponding holmium(III) compounds are not liquid crystalline.

Introduction

Although the first papers on lanthanide(III) alkanooates were published in the early 1960s,^{1,2} the mesomorphic behavior of these compounds was only discovered in 1998. Marques et al. found that cerium(III) alkanooates are mesomorphic and that the phase behavior depends on the alkyl chain length. Whereas the short-chain cerium homologues show several mesophases, only one mesophase is present for complexes with longer alkyl chains.³ However, the exact mesophase could not be determined although the authors suggested a layered mesophase. Binnemans et al. confirmed the mesophase behavior.⁴ They found for lanthanum(III) tetradecanoate and longer homologues a smectic A phase. Lanthanide(III) alkanooates adopt a lamellar bilayer structure whereby the alkyl chains are placed perpendicular to the ionic lanthanide layer.

Jongen et al. made a systematic study of lanthanide(III) alkanooates.^{5–10} It was found that the size of the lanthanide ion has a critical effect on the existence of a

mesophase. In the case of lanthanide(III) dodecanoates a mesophase is only present for the large lanthanide ions (i.e., La^{III}, Ce^{III}, Pr^{III}, and Nd^{III}). Also, the chain length influences the thermal behavior of lanthanide soaps. For lanthanum(III), cerium(III), and praseodymium(III) alkanooates, two mesophases are present for the short chain homologues and one mesophase is present for the long chain homologues. In contrast, the neodymium(III) alkanooates do not exhibit a mesophase for the very long alkyl chain lengths.

4-Alkoxybenzoic acids are well-known for their mesomorphic behavior.^{11–19} The compounds with a short terminal alkyl chain exhibit a nematic phase, and those with intermediate chain lengths show both a nematic and a smectic C phase; whereas compounds with very long alkyl chains show a smectic C phase only. Information on lanthanide complexes of 4-alkoxybenzoic acids is really scarce, except for some papers on the synthesis and structure of lanthanide(III) benzoates and derivatives thereof.^{20–23}

* Corresponding author. Fax: +32 16 32 7992. E-mail: koen.binnemans@chem.kuleuven.ac.be.

[†] Katholieke Universiteit Leuven.

[‡] DUBBLE-CRG/ESRF.

(1) Misra, S. N.; Misra, T. N.; Mehrotra, R. C. *J. Inorg. Nucl. Chem.* **1963**, *25*, 195.

(2) Misra, S. N.; Misra, T. N.; Mehrotra, R. C. *J. Inorg. Nucl. Chem.* **1963**, *25*, 201.

(3) Marques, E. F.; Burrows, H. D.; da Graça Miguel, M. *J. Chem. Soc., Faraday Trans.* **1998**, *94*, 1729.

(4) Binnemans, K.; Heinrich, B.; Guillon, D.; Bruce, D. W. *Liq. Cryst.* **1999**, *26*, 1717.

(5) Binnemans, K.; Jongen, L.; Görrler-Walrand, C.; D'Olieslager, W.; Hinz, D.; Meyer, G. *Eur. J. Inorg. Chem.* **2000**, 1429.

(6) Binnemans, K.; Jongen, L.; Bromant, C.; Hinz, D.; Meyer, G. *Inorg. Chem.* **2000**, *39*, 5938.

(7) Jongen, L.; Binnemans, K.; Hinz, D.; Meyer, G. *Liq. Cryst.* **2001**, *28*, 819.

(8) Jongen, L.; Binnemans, K.; Hinz, D.; Meyer, G. *Mater. Sci. Eng. C* **2001**, *18*, 199.

(9) Jongen, L.; Binnemans, K.; Hinz, D.; Meyer, G. *Liq. Cryst.* **2001**, *28*, 1727.

(10) Jongen, L.; Hinz, D.; Meyer, G.; Binnemans, K. *Chem. Mater.* **2001**, *13*, 2243.

(11) Herbert, A. J. *Trans. Faraday Soc.* **1967**, *63*, 555.

(12) Blumstein, A.; Platel, L. *Mol. Cryst. Liq. Cryst.* **1978**, *48*, 151.

(13) Gray, G. W.; Jones, B. J. *Chem. Soc.* **1953** 4179.

(14) Bryan, R. F.; Hartley, P.; Miller, R. W.; Shen, M. S. *Mol. Cryst. Liq. Cryst.* **1980**, *62*, 281.

(15) Bryan, R. F.; Hartley, P. *Mol. Cryst. Liq. Cryst.* **1980**, *62*, 259.

(16) Babkov, L. M.; Gorshkov, O. V.; Golovina, N. A.; Puchkovskay, G. A.; Khakimov, I. N. *J. Struct. Chem.* **1995**, *36*, 302.

(17) Kato, T.; Kubota, Y.; Nakano, M.; Uryu, T. *Chem. Lett.* **1995**, 1127.

(18) Plass, M. Z. *Phys. Chem. Int. Ed.* **1996**, *194*, 223.

(19) Painter, P.; Cleveland, C.; Coleman, M. *Mol. Cryst. Liq. Cryst.* **2000**, *348*, 269.

Experimental Section

Equipment. CH elemental microanalyses were performed on a CE Instruments EA-1110 elemental analyzer. The agreement between experimental and theoretical values had to be within $\pm 0.5\%$.

Differential scanning calorimetry (DSC) data were collected on a Mettler-Toledo DSC 821e-module. Solid samples of 2–5 mg were put in sealed aluminum crucibles (40 μL) with a pierced lid and were heated or cooled at a scan rate of $10\text{ }^{\circ}\text{C min}^{-1}$ under a helium flow (40 mL min^{-1}). Indium metal was used as standard for the calibration of the instrument ($T_m = 156.6 \pm 0.3\text{ }^{\circ}\text{C}$, $\Delta H_m = 28.45 \pm 0.6\text{ J g}^{-1}$).

Optical textures were observed with an Olympus BX60 polarizing optical microscope equipped with a Linkam THMS 600 hot stage and a Linkam TMS 93 programmable temperature-controller. The heating rate ranged between 2 and $10\text{ }^{\circ}\text{C min}^{-1}$.

Synchrotron X-ray measurements were done on the DUBBLE-beamline (BM 26) at the European Synchrotron Radiation Facility (ESRF) in Grenoble, France.^{24–25} Intensities at scattering angles between 0.39 and 15° were collected on a quadrant type detector²⁶ at 0.5 m from the sample. Distances in real space between 100 and 2.7 \AA could be covered by using an X-ray wavelength, $\lambda = 0.6889\text{ \AA}$. Data were corrected for the detector response and normalized to the intensity of the primary beam, measured at the detector position. The scattering angles were calibrated using the reflections of $\text{La}(\text{C}_{11}\text{H}_{23}\text{CO}_2)_3$ at room temperature. The d values, obtained for a bilayered structure with the alkyl chains perpendicular to the ionic layer and in the *all trans* conformation, were taken from Jongen et al.⁵ Data are represented as a function of s , with $s = 2\sin\theta/\lambda$ and θ half the scattering angle. No corrections were done to account for the use of a flat detector. Flat samples of 1 mm thick, placed in a brass mold and covered by aluminum foil, were mounted in a Mettler FP82-HT hot stage, and flushed with nitrogen for temperature control. The heating rate used was $10\text{ }^{\circ}\text{C min}^{-1}$ throughout. Scattering patterns were collected sequentially during 6 s , corresponding to one pattern for each degree centigrade in the temperature ramp.

Synthesis. Reagents and solvents were used as received without further purification. Analytical grade solvents were used for the synthesis and washing of the complexes. Hydrated lanthanide(III) nitrates were purchased from Aldrich. The 4-alkoxybenzoic acids were prepared via a Williamson-ether synthesis, by reaction during 48 h of the corresponding *n*-bromoalkane with a mixture of ethyl-4-hydroxybenzoate and potassium carbonate, using potassium iodide as the catalyst and 2-butanone as the solvent. This was followed by saponification of the ester and workup in acidic solution. The 4-alkoxybenzoic acid was recrystallized from absolute ethanol. In this way the following 4-alkoxybenzoic acids were synthesized: 4-butyloxybenzoic acid, 4-hexyloxybenzoic acid, 4-octyloxybenzoic acid, 4-nonyloxybenzoic acid, and 4-decyloxybenzoic acid.

Synthesis of 4-Butyloxybenzoic Acid. *n*-Bromobutane (0.10 mol , 13.75 g), ethyl-4-hydroxybenzoate (0.10 mol , 16.62 g), and potassium carbonate (0.4 mol , 55.28 g) were dissolved in 300 mL of 2-butanone. A small amount potassium iodide was added as the catalyst. This mixture was refluxed for 48 h , and after it was cooled to room temperature 800 mL of water was added. The water layer was washed three times with

diethyl ether; the organic layer was washed with water (twice) and brine. The organic solutions were dried over MgSO_4 and the solvent was removed. The liquid was dissolved in 250 mL of ethanol and NaOH was added (0.16 mol , 6.40 g). This was refluxed for 2.5 h . The mixture was poured in an acidic water solution ($\text{pH} = 1$, HCl). The precipitate was filtrated and washed thoroughly in water. The crude product was recrystallized from absolute ethanol. Yield: 9.56 g , 74% .

CH analysis for $\text{C}_4\text{H}_9\text{OC}_6\text{H}_4\text{CO}_2\text{H}$: experimental for C, 68.02% ; H, 7.27% ; calculated for C, 68.02% ; H, 7.32% . $^1\text{H NMR}$ for $\text{C}_4\text{H}_9\text{OC}_6\text{H}_4\text{CO}_2\text{H}$ (250 MHz , CDCl_3 , δ ppm): 0.95 (t, 3H, CH_3); 1.48 (m, 2H, $\text{CH}_3\text{--CH}_2\text{--CH}_2\text{--}$); 1.78 (quintet, 2H, $\text{CH}_3\text{--CH}_2\text{--CH}_2\text{--}$); 4.01 (t, 2H, $\text{--CH}_2\text{--CH}_2\text{--O}$); 6.91 (dd, 2H, H-aryl, $J_o = 6\text{ Hz}$); 8.02 (dd, 2H, H-aryl, $J_o = 9\text{ Hz}$). Analogous analysis and NMR results were obtained for the other 4-alkoxybenzoic acids.

Synthesis of the Complexes. Lanthanide(III) 4-alkoxybenzoates were prepared via a metathesis reaction between the sodium salt of a 4-alkoxybenzoic acid and the corresponding lanthanide(III) nitrate. To a solution of a 4-alkoxybenzoic acid in ethanol an equivalent amount of NaOH was added. To this sodium salt an aqueous solution of the desired lanthanide(III) nitrate was added dropwise. The metal complex immediately precipitated. After the mixture was stirred for 1 h the precipitate was filtered off and dried in a vacuum. Complexes were synthesized of 4-butyloxybenzoic acid, 4-hexyloxybenzoic acid, 4-octyloxybenzoic acid, 4-nonyloxybenzoic acid, and 4-decyloxybenzoic acid with La^{III} and Ho^{III} . The compounds were obtained as waxy parchment art fragments with the typical color of the corresponding trivalent lanthanide ion.²⁷ Most of the lanthanide(III) 4-alkoxybenzoates were di- or trihydrates. The voluminous headgroups of the ligands can explain the high degree of hydration of these complexes. This causes much space in the first and second coordination sphere of the lanthanide ion, where water molecules can be placed and hence give rise to hydrated complexes. Results obtained for $\text{Ho}(\text{C}_6\text{H}_{13}\text{OC}_6\text{H}_4\text{CO}_2)_3 \cdot 3\text{H}_2\text{O}$: experimental for C, 53.19% ; for H, 6.36% ; calculated for C, 53.06% ; for H, 6.51% .

Results and Discussion

The thermal behavior of the lanthanide(III) 4-alkoxybenzoates is quite complicated in the sense that depending on the lanthanide ion and on the chain length different solid-state and/or mesophase structures are observed. A common feature among all these structures is that they consist of layers. First, an overview will be given of the different possible layered structures for the compounds presented in this study (Figures 1–3). The actual structural assignment, which is presented below, is based on a combined treatment of the DSC-thermograms, the textures observed by thermooptical microscopy, and X-ray diffraction.

A normal layered structure (structure 1 in Figure 1) with characteristic interlayer distance d_l , gives rise to higher order reflections at angles that correspond to distances calculated with Bragg's law as $d/2$, $d/3$, ..., d/n . In this structure, the molecules are fully stretched. This structure is often observed for the normal solid lanthanide(III) alkanoates at room temperature.^{5–10}

Similar higher orders peaks are also possible for a smectic A and a smectic C structure and for intercalated smectic structures (respectively structures 2, 3, and 4 in Figure 1). However for these structures the d values change under influence of the temperature. In a smectic A structure, the d value decreases at increasing temperature, whereas the d value of a smectic C structure

(20) Kula, A.; Brzyska, W. *Polish J. Chem.* **2000**, *74*, 45.

(21) Keli, Z.; Jibing, Y.; Liangjie, Y.; Jutang, S. *J. Rare Earths* **1999**, *17*, 255.

(22) Taylor, M. D.; Carter, C. P.; Wynter, C. I. *J. Inorg. Nucl. Chem.* **1968**, *30*, 1503.

(23) Ferenc, W.; Bocian, B.; Mazur, D. *Croatica Chimica Acta* **1999**, *72*, 779.

(24) Borsboom, M.; Bras, W.; Cerjak, I.; Detollenaere, D.; Glastra van Loon, D.; Goedtkindt, P.; Konijnenburg, M.; Lassing, P.; Levine, Y. K.; Munneke, B.; Oversluizen, M.; van Tol, R.; Vlieg, E. *J. Synchro. Rad.* **1998**, *5*, 518.

(25) Bras, W. *J. Macromol. Sci. Phys.* **1998**, *B37*, 557.

(26) Gabriel, A.; Dauvergne, F. *Nucl. Instr. Meth.* **1982**, *201*, 223.

(27) Binnemans, K.; Görrler-Walrand, C. *Chem. Phys. Lett.* **1995**, *235*, 163.

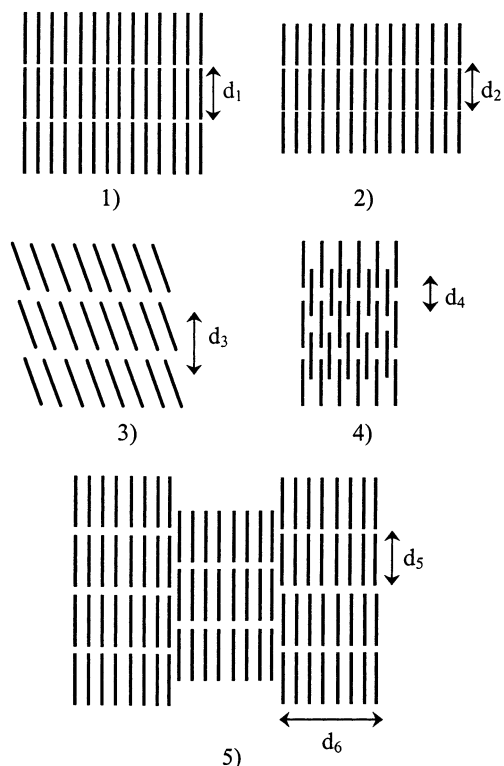


Figure 1. Schematic representations of different types of layered structures: (1) normal layered structure, molecules are fully stretched; (2) smectic A structure, molecules are not fully stretched; (3) smectic C structure; (4) intercalated smectic structure ($d_1 > d_2, d_3, d_4$); (5) modulated $\text{Sm}\bar{\text{A}}$.

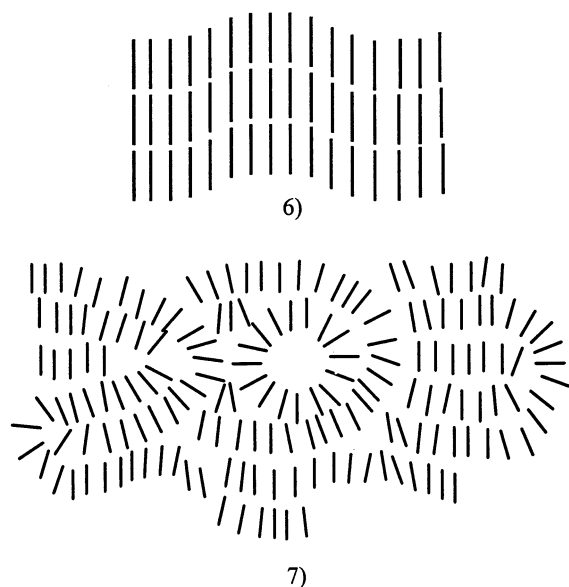


Figure 2. Schematic representation of less ordered structures: (6) undulating layered structure; (7) random domains.

increases.²⁸ In these mesophase structures the molecules are not fully stretched.

Modulated smectic phases (structure 5 in Figure 1), denoted as modulated $\text{Sm}\bar{\text{A}}$ mesophases, are built by biaxial ribbons, which is clearly visible in their diffraction pattern. Diffraction patterns of compounds with

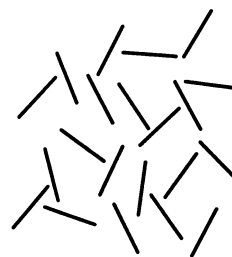


Figure 3. Schematic representation of the isotropic state, with a total random orientation of the molecules.

this structure show, apart from the diffraction peak of the layers (d_5), a second peak at higher d values.²⁸ This peak is related to the width of the ribbons (d_6).

This type of smectic mesophase has been observed for mesogens having strongly polar end groups.^{29,30} However, in this discussion we have used the structure of the modulated smectic A phase for the description of solid, crystalline compounds. In the $\text{Sm}\bar{\text{A}}$ structure for solid, crystalline compounds the molecules are in their *all trans* conformation, whereas in a normal $\text{Sm}\bar{\text{A}}$ mesophase the molecules are not fully stretched. The presence of this modulated $\text{Sm}\bar{\text{A}}$ structure is very probable for lanthanide(III) 4-alkoxybenzoates, because steric effects can also induce these structure.²⁸

The main difference between the structures described above and both the undulating layered structure (structure 6 in Figure 2) and the structure with random domains (structure 7 in Figure 2) is that for the latter two structures higher order peaks are less probable. For the undulating layered structure a peak at higher d value is probable and is due to the undulation. In the case of a structure with random domains, scattering peaks are rather broad. When total randomization occurs (Figure 3), no peak is observed. Whereas for structures 2–6 birefringence is possible in thermo-optical microscopy, no birefringence is observed for the structure with random domains and the total random phase, because of their isotropy.

In the case of lanthanide(III) 4-alkoxybenzoates the layers are actually bilayers, whereby on both sides of the ionic lanthanide and carboxylate layer the organic tail of the 4-alkoxybenzoates is placed. This means that in the case of a normal layered structure (structure 1), the layer distance d_1 is approximately twice the length of the 4-alkoxybenzoic acid.

Clearly the chain length has an influence on the thermal behavior of lanthanum(III) 4-alkoxybenzoates. The differences can be accounted for by considering structural differences at room temperature.

$\text{La}(\text{C}_4\text{H}_9\text{OC}_6\text{H}_4\text{CO}_2)_3$ shows in DSC two transitions in the first heating run, whereby the enthalpy change of the first transition is much larger than that of the second. In principle this could point to a mesophase. In thermo-optical microscopy this compound shows some birefringence, but no fluidity, casting doubt on the mesophase hypothesis and pointing to a crystal–crystal transition, which is plausible because of the short alkyl chains involved. By X-ray diffraction measurements we were able to attach the modulated $\text{Sm}\bar{\text{A}}$ structure on

(28) Seddon, J. M. In *Handbook of Liquid Crystals*; Demus, D.; Goodby, J.; Gray, G. W.; Spiess, H.-W., Eds. VCH–Wiley, Weinheim: New York, 1998; Vol. 1 Chapter 3.

(29) Ostrovskii, B. I. *Liq. Cryst.* **1993**, *14*, 131.

(30) Lobko, T. A.; Ostrovskii, B. I.; Pavluchenko, A. I.; Sulianov, S. N. *Liq. Cryst.* **1993**, *15*, 361.

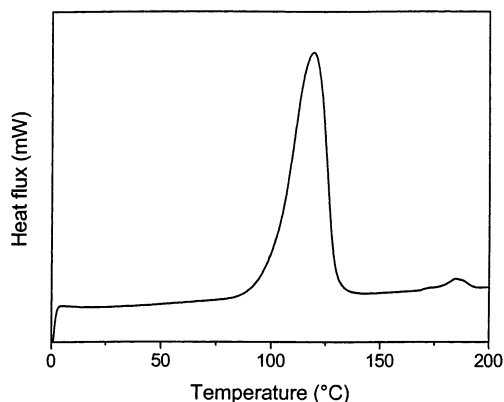


Figure 4. DSC-thermograms of $\text{La}(\text{C}_6\text{H}_{13}\text{OC}_6\text{H}_4\text{CO}_2)_3$, endothermic peaks are pointing upward.

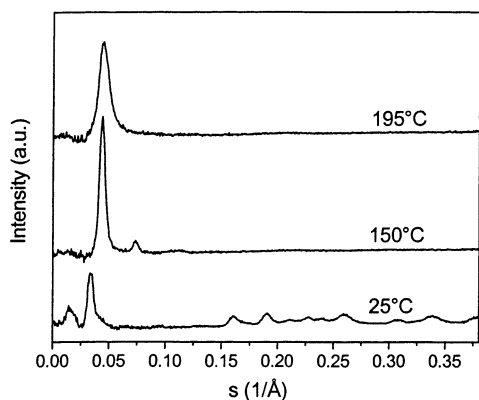


Figure 5. X-ray diffractograms of $\text{La}(\text{C}_6\text{H}_{13}\text{OC}_6\text{H}_4\text{CO}_2)_3$ at different temperatures.

the room-temperature solid, crystalline phase (structure 5). At the first transition the lanthanum(III) 4-butyl-oxybenzoate rearranges to a solid structure with undulating layers (structure 6). Finally, the compound melts to an isotropic, liquid structure with random domains (structure 7).

In the case of $\text{La}(\text{C}_6\text{H}_{13}\text{OC}_6\text{H}_4\text{CO}_2)_3$, $\text{La}(\text{C}_8\text{H}_{17}\text{OC}_6\text{H}_4\text{CO}_2)_3$, and $\text{La}(\text{C}_9\text{H}_{19}\text{OC}_6\text{H}_4\text{CO}_2)_3$ a mesophase is formed at heating a fresh sample. In Figure 4 the DSC thermogram of lanthanum(III) 4-hexyloxybenzoate is given. Although this thermogram is very similar to that of the 4-butyl-oxybenzoate homologue, the behavior in thermooptical microscopy and X-ray diffraction is different. The compounds show textures comparable to those observed for the lanthanide(III) alkanoates.^{3–9} Most often the textures had a grainy appearance with white-yellow zones on a dark background. The compounds are not very fluid. In Figure 5 the X-ray diffractograms of $\text{La}(\text{C}_6\text{H}_{13}\text{OC}_6\text{H}_4\text{CO}_2)_3$ at different temperatures are given. The lanthanum(III) 4-hexyloxybenzoate shows at room temperature a complex type of a solid, biaxial $\text{Sm}\bar{\text{A}}$ structure, i.e., a modulated $\text{Sm}\bar{\text{A}}$ structure. This is visible in the appearance of a diffraction peak of this compound at high d values. At the first phase transition, the modulated $\text{Sm}\bar{\text{A}}$ structure disappears. The compound still shows a layered structure, but the d value decreases because of melting of the alkyl chains. Combination of the results obtained by the three techniques confirms the suspicion of a mesophase. X-ray data reveal the presence of a smectic A mesophase (structure 2 in Figure 2). Higher order peaks are observed and nominally infinite layers are formed (Figure 5).

Table 1. Transition Temperatures and Enthalpies for the Series $\text{La}(\text{C}_x\text{H}_{2x+1}\text{OC}_6\text{H}_4\text{CO}_2)_3$

compound	transition ^a	T (°C)	ΔH (kJ mol ⁻¹)
$\text{La}(\text{C}_4\text{H}_9\text{OC}_6\text{H}_4\text{CO}_2)_3$	5 \rightarrow 6	117	119
	6 \rightarrow 7	266	24.7
$\text{La}(\text{C}_6\text{H}_{13}\text{OC}_6\text{H}_4\text{CO}_2)_3$	5 \rightarrow 2	119	119
	2 \rightarrow 7	185	2.80
$\text{La}(\text{C}_8\text{H}_{17}\text{OC}_6\text{H}_4\text{CO}_2)_3$	5 \rightarrow 2	117	162
	2 \rightarrow 7	171	1.21
$\text{La}(\text{C}_9\text{H}_{19}\text{OC}_6\text{H}_4\text{CO}_2)_3$	5 \rightarrow 2	117	196
	2 \rightarrow 7	167	1.28
$\text{La}(\text{C}_{10}\text{H}_{21}\text{OC}_6\text{H}_4\text{CO}_2)_3$	5 \rightarrow 7	120	172

^a The numbers refer to the structures described in Figures 1–3, structure 2 corresponds to a smectic A phase.

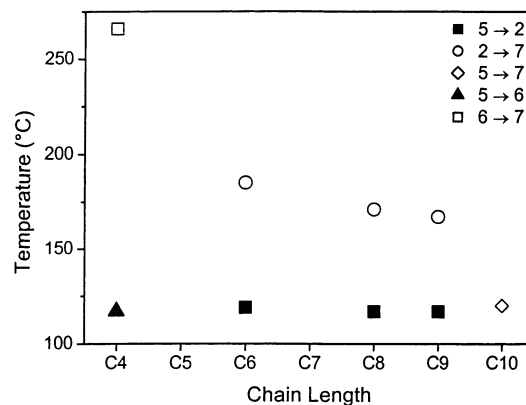


Figure 6. Phase diagram of the series $\text{La}(\text{C}_x\text{H}_{2x+1}\text{OC}_6\text{H}_4\text{CO}_2)_3$; numbers refer to the structures described in Figures 1–3. The compounds are labeled with the number of carbon atoms in the alkyl chain, e.g. C6 stands for $\text{La}(\text{C}_6\text{H}_{13}\text{OC}_6\text{H}_4\text{CO}_2)_3$.

At 185 °C there is no shift in d value but the peak broadens. Here the synchrotron X-ray data show still some structure, although in thermooptical microscopy no birefringence is observed. This means that not all the structure is lost, but that some random domains remain (structure 7).

By the three techniques, only one transition could be observed for $\text{La}(\text{C}_{10}\text{H}_{21}\text{OC}_6\text{H}_4\text{CO}_2)_3$ (Table 1). At room temperature the modulated $\text{Sm}\bar{\text{A}}$ structure can be assigned to the solid compound. At 120 °C lanthanum(III) 4-decyloxybenzoate melts to a structure with random domains. In Figure 6 the phase diagram of the series $\text{La}(\text{C}_x\text{H}_{2x+1}\text{OC}_6\text{H}_4\text{CO}_2)_3$ is given.

The thermal behavior of the holmium(III) 4-alkoxybenzoates is different from that of the corresponding lanthanum(III) compounds. $\text{Ho}(\text{C}_4\text{H}_9\text{OC}_6\text{H}_4\text{CO}_2)_3$ shows in DSC a weak transition at 69 °C and a stronger one at 193 °C. From X-ray diffraction it was clear that this compound is amorphous in the solid state and changes to a structure with random domains at ca. 195 °C (Figure 7).

$\text{Ho}(\text{C}_6\text{H}_{13}\text{OC}_6\text{H}_4\text{CO}_2)_3$, $\text{Ho}(\text{C}_8\text{H}_{17}\text{OC}_6\text{H}_4\text{CO}_2)_3$, $\text{Ho}(\text{C}_9\text{H}_{19}\text{OC}_6\text{H}_4\text{CO}_2)_3$, and $\text{Ho}(\text{C}_{10}\text{H}_{21}\text{OC}_6\text{H}_4\text{CO}_2)_3$ show in DSC, thermooptical microscopy, and X-ray diffraction a comparable set of transitions. DSC-thermograms display two endothermic peaks at heating a fresh sample. The enthalpy of the first transition is much larger than that of the second one (Figure 8 and Table 2), indicating a mesophase. However, in the temperature window between both transitions the compounds do not show any fluidity, although in thermooptical microscopy some birefringence appears. On the basis of

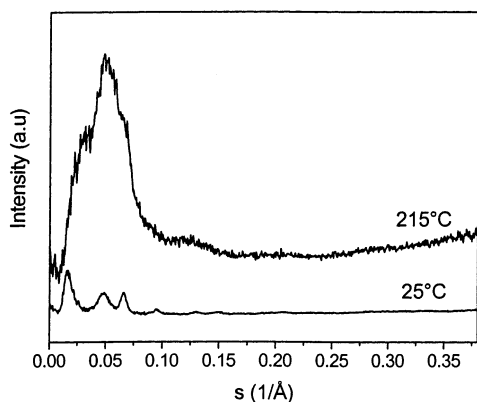


Figure 7. X-ray diffractograms of $\text{Ho}(\text{C}_4\text{H}_9\text{OC}_6\text{H}_4\text{CO}_2)_3$ at different temperatures.

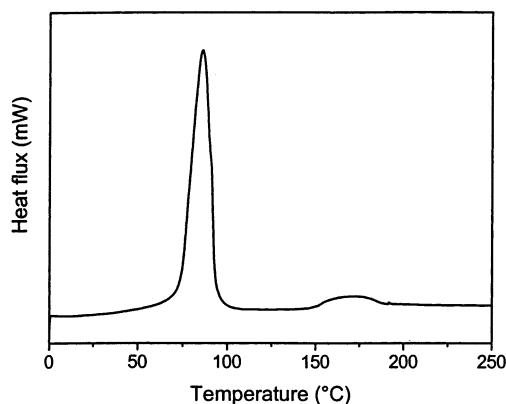


Figure 8. DSC-thermograms of $\text{Ho}(\text{C}_8\text{H}_{17}\text{OC}_6\text{H}_4\text{CO}_2)_3$; endothermic peaks are pointing upward.

Table 2. Transition Temperatures and Enthalpies for the Series $\text{Ho}(\text{C}_x\text{H}_{2x+1}\text{OC}_6\text{H}_4\text{CO}_2)_3$

compound	transition ^a	<i>T</i> (°C)	ΔH (kJ mol ⁻¹)
$\text{Ho}(\text{C}_4\text{H}_9\text{OC}_6\text{H}_4\text{CO}_2)_3$	5 \rightarrow 6	(69)	(3.01)
	6 \rightarrow 7	193	22.09
$\text{Ho}(\text{C}_6\text{H}_{13}\text{OC}_6\text{H}_4\text{CO}_2)_3$	5 + 6 \rightarrow 6	94	71
	6 \rightarrow 7	160	7.62
$\text{Ho}(\text{C}_8\text{H}_{17}\text{OC}_6\text{H}_4\text{CO}_2)_3$	5 + 6 \rightarrow 6	86	109
	6 \rightarrow 7	170	8.12
$\text{Ho}(\text{C}_9\text{H}_{19}\text{OC}_6\text{H}_4\text{CO}_2)_3$	5 + 6 \rightarrow 6	94	66
	6 \rightarrow 7	161	7.01
$\text{Ho}(\text{C}_{10}\text{H}_{21}\text{OC}_6\text{H}_4\text{CO}_2)_3$	5 + 6 \rightarrow 6	88	118
	6 \rightarrow 7	168	3.08

^a The numbers refer to the structures described in Figures 1–3.

these results only, one may be tempted to identify the first transition as a crystal–crystal transition. However, X-ray data offer another explanation as they reveal the presence of two different structures at room temperature, i.e. structure 5 and structure 6 (respectively the modulated Sm $\bar{\text{A}}$ structure and the undulating layered structure). In Figure 9 scattering patterns of $\text{Ho}(\text{C}_8\text{H}_{17}\text{OC}_6\text{H}_4\text{CO}_2)_3$ at different temperatures are given. The low angle peak at $s = 0.015 \text{ \AA}^{-1}$ for the pattern at 25 °C is most likely a superposition of the two low angle peaks associated with the two different structures. The second peak at slightly higher s values is clearly a double peak, originating from two layered structures ($s = 0.031 \text{ \AA}^{-1}$ and $s = 0.040 \text{ \AA}^{-1}$), with the one at $s = 0.031 \text{ \AA}^{-1}$ belonging to the pattern of the modulated Sm $\bar{\text{A}}$ structure. At the first phase transition the peak at $s = 0.031 \text{ \AA}^{-1}$ disappears. The intensity of the peak at $s = 0.040 \text{ \AA}^{-1}$ increases. This means that the part of

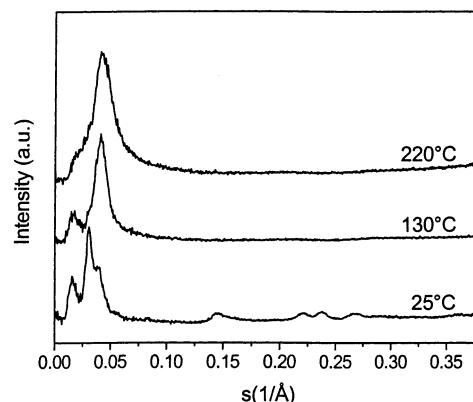


Figure 9. X-ray diffractograms of $\text{Ho}(\text{C}_8\text{H}_{17}\text{OC}_6\text{H}_4\text{CO}_2)_3$ at different temperatures.

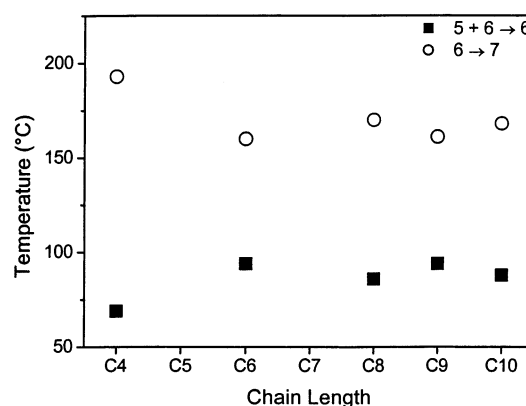


Figure 10. Phase diagram of the series $\text{Ho}(\text{C}_x\text{H}_{2x+1}\text{OC}_6\text{H}_4\text{CO}_2)_3$, numbers refer to the structures described in Figures 1–3. The compounds are labeled with the number of carbon atoms in the alkyl chain; e.g., C6 stands for $\text{Ho}(\text{C}_6\text{H}_{13}\text{OC}_6\text{H}_4\text{CO}_2)_3$.

the compound originally in structure 5 rearranges to structure 6. So the complete bulk shows the undulating layered structure in the second phase. At the second phase transition the compounds clear into the structure with random domains. $\text{Ho}(\text{C}_6\text{H}_{13}\text{OC}_6\text{H}_4\text{CO}_2)_3$, $\text{Ho}(\text{C}_9\text{H}_{19}\text{OC}_6\text{H}_4\text{CO}_2)_3$, and $\text{Ho}(\text{C}_{10}\text{H}_{21}\text{OC}_6\text{H}_4\text{CO}_2)_3$ show a similar behavior in X-ray diffraction. In Figure 10 the phase diagram of the series $\text{Ho}(\text{C}_x\text{H}_{2x+1}\text{OC}_6\text{H}_4\text{CO}_2)_3$ is given.

Complexes of 4-alkoxybenzoic acids do not crystallize when cooling from the phase with random domains. During the first heating of fresh products the layered structure is broken down into a less-ordered layered structure with random domains. Because of the strong steric hindrance due to the phenyl groups, it is very difficult to restore the layered structure during subsequent cooling, and the structure will remain more or less random (i.e., the same structure as formed at the last phase transition). At cooling, the motion of the molecules will diminish gradually. No exothermic peak is present in DSC, and neither is a change in d spacing in diffraction measurements. This gradual process is reversible in the sense that in the second heating run no transition can be seen in DSC and X-ray diffraction, although softening of the compounds is observed in thermo-optical microscopy.

Conclusions

Both the lanthanide ion and the alkyl chain length have an influence on the thermal behavior of lanthani-

de(III) 4-alkoxybenzoates. From synchrotron X-ray diffraction it was clear that compounds of the series $\text{La}(\text{C}_x\text{H}_{2x+1}\text{OC}_6\text{H}_4\text{CO}_2)_3$ and $\text{Ho}(\text{C}_x\text{H}_{2x+1}\text{OC}_6\text{H}_4\text{CO}_2)_3$ crystallize during synthesis in a different form depending on the lanthanide ion, and, for the corresponding holmium(III) compounds, the length of the alkyl chain. For the lanthanum(III) series, all the compounds form a modulated $\text{Sm}\tilde{\text{A}}$ phase. $\text{La}(\text{C}_6\text{H}_{13}\text{OC}_6\text{H}_4\text{CO}_2)_3$, $\text{La}(\text{C}_8\text{H}_{17}\text{OC}_6\text{H}_4\text{CO}_2)_3$, and $\text{La}(\text{C}_9\text{H}_{19}\text{OC}_6\text{H}_4\text{CO}_2)_3$ form a mesophase at the first heating run. However, the formation of a mesophase is due to the melting of the alkyl chain of the 4-alkoxybenzoate, rather than a rearrangement of the rigid layer where the lanthanide ions, the carboxylate groups, and the phenyl groups are situated. This gives rise to a mesophase with molten alkyl chains but with restricted movement through the ionic layer. The 4-butyloxybenzoate homologue has an alkyl chain that is too short to form a stable mesophase. In the case of the 4-decyloxybenzoate the layered structure breaks down before the alkyl chains are completely molten. The fact that some of the lanthanum(III) homologues are mesomorphic means that the lanthanum ion is large enough to stabilize unfavorable interactions between the carboxylate and/or phenyl groups.

Although most of the holmium(III) homologues also show a modulated $\text{Sm}\tilde{\text{A}}$ structure at room temperature,

none of this series is mesomorphic. The holmium(III) ion is much smaller than the lanthanum(III) ion and is not large enough to stabilize the ionic layer with a close packing of carboxylate and phenyl groups. The modulated $\text{Sm}\tilde{\text{A}}$ structure is no longer stable during heating and will rearrange to a structure with undulating layers.

This dependence of a mesophase on the size of the lanthanide ion has also been observed for the normal lanthanide(III) alkanoates.⁵

Acknowledgment. L.J. is indebted to the Institute for the Promotion of Innovation by Science and Technology in Flanders (IWT). K.B. thanks the FWO-Flanders (Belgium) for a postdoctoral fellowship and a research grant (G.0243.99). B.G. is indebted to the Research Council of the K. U. Leuven for a postdoctoral fellowship. The authors thank FWO-Flanders and Prof. H. Reynaers for their continuous support of the DUBBLE project.

Supporting Information Available: Tables of chemical analysis results and transition temperatures of the 4-alkoxybenzoic acids; tables of chemical analysis results of the lanthanum(III) 4-alkoxybenzoates and of the holmium(III) alkoxybenzoates. This material is available free of charge via the Internet at <http://pubs.acs.org>.

CM0212461